Journal Pre-proof

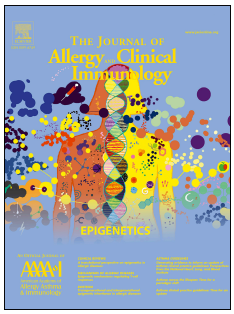

Vagal sensory neurons drive mucous cell metaplasia

Sébastien Talbot, PhD, Benjamin Doyle, MSc, Junwei Huang, PhD, Jo-Chiao Wang, MSc, Maryam Ahmadi, MSc, David P. Roberson, PhD, Ajay Yekkirala, PhD, Simmie L. Foster, MD, PhD, Liam E. Browne, PhD, Bruce P. Bean, PhD, Bruce D. Levy, MD, Clifford J. Woolf, MB, BCh, PhD

PII: S0091-6749(20)30037-3

DOI: https://doi.org/10.1016/j.jaci.2020.01.003

Reference: YMAI 14367

To appear in: *Journal of Allergy and Clinical Immunology*

Received Date: 25 September 2019

Revised Date: 21 December 2019

Accepted Date: 2 January 2020

Please cite this article as: Talbot S, Doyle B, Huang J, Wang J-C, Ahmadi M, Roberson DP, Yekkirala A, Foster SL, Browne LE, Bean BP, Levy BD, Woolf CJ, Vagal sensory neurons drive mucous cell metaplasia, *Journal of Allergy and Clinical Immunology* (2020), doi: https://doi.org/10.1016/j.jaci.2020.01.003.

Vagal sensory neurons drive mucous cell metaplasia

Sébastien Talbot, *PhD* [a,b,c,*], Benjamin Doyle, *MSc* [a,b], Junwei Huang, *PhD* [a,b], Jo-Chiao Wang, *MSc* [c], Maryam Ahmadi, *MSc* [c], David P. Roberson, *PhD* [a,b], Ajay Yekkirala, *PhD* [a,b], Simmie L. Foster, *MD, PhD* [a,b], Liam E. Browne, *PhD* [a,b,e], Bruce P. Bean, *PhD* [b], Bruce D. Levy, *MD* [d], and Clifford J. Woolf, *MB, BCh, PhD* [a, b,*]

[a] FM Kirby Neurobiology Center, Children's Hospital Boston, Boston, USA.
[b] Department of Neurobiology, Harvard Medical School, Boston, USA.
[c] Département de Pharmacologie et Physiologie, Université de Montréal, Montréal, Canada.
[d] Pulmonary and Critical Care Medicine Division, Department of Internal Medicine, Brigham and Women's Hospital, Harvard Medical School, Boston, USA.
[e] Wolfson Institute for Biomedical Research, University College London, London, UK.

*Corresponding authors:
Clifford J. Woolf, MB, BCh, PhD
Tel.: 617-919-2393. Fax: 617-919-2772
E-Mail address: clifford.woolf@childrens.harvard.edu

Sebastien Talbot. PhD
Tel.: 514-343-6111. Fax: 514-343-2111
E-Mail address: sebastien.talbot@umontreal.ca

Running title: Sensory neurons drive mucous metaplasia

Key words: Vagal sensory neurons; TRPV1; QX-314; Optogenetic; Mucous metaplasia; Goblet cell hyperplasia; Substance P; Muc5AC; Muc5B; Asthma.

Capsule summary. Airway sensory neuron-produced Substance P heightens allergy-induced goblet cell hyperplasia and hypersecretion of Muc5AC, electrically silencing these overreactive neurons reduced these components of lung type 2 allergic inflammatory response.

To the editor,

By trapping inhaled pathogens and toxic particulates, the mucus lining of the airways fulfills an important protective contribution to innate immune function (1). Mucus clearance or accumulation depends on the balance between mucin production and its elimination, providing either an effective defense barrier or disease favoring mucus excess (1). Mucus is largely composed of mucins which are high molecular weight heavily glycosylated proteins. They are encoded by MUC genes and segregate into three major families: secreted gel-forming (Muc5AC, Muc5B); membrane-associated; and non–gel-forming secreted mucin (2). While the functions of mucin subtypes are not well understood, membrane-associated mucins can act as receptors for invading pathogens and initiate innate immune responses, while secreted mucins prevent epithelial inflammation (2). Muc5AC contributes to airway hyperactivity (3), a key feature of asthma and Muc5B to mucociliary clearance, immune homeostasis, and airway inflammation resolution (4). In patients with severe asthma, lung airway Muc5B expression is decreased by up to 90%, while Muc5AC expression is highly upregulated (4).

Sensory neurons drive mucus hyperplasia.

The nature and mechanisms responsible for the protective role of mucins in preventing airway diseases in health, and the changes in secreted mucins and its clearance failure in disease, require further exploration. There are suggestions that the nervous system influences mucus production, and this may provide a way to intervene therapeutically. Circadian rhythms, through vagal nerve signaling, are primary regulators of submucosal gland activation (5). We previously uncovered that vagal sensory neurons amplify ILC2 and $CD4^+$ T cells activation, driving a pro-inflammatory loop between these neurons and airway immune cells (6). To probe for a role of vagal sensory neurons in mucus production we used optogenetics via cre-loxp targeted channelrhodopsin (ChR2) expression in vagal sensory ($TRPV1^{cre/wt}$::$ChR2^{fl/wt}$ and $Tac1^{cre/wt}$::$ChR2^{fl/wt}$) or motor neurons ($ChAT^{ChR2}$-eYFP). Acute optogenetic stimulation of the vagus nerve trunk (3.5 ms, 5Hz, 473nm, 100 mW, giving approx. 2-6 mW/mm^2 with a 0.39 NA fiber placed 5-10 mm from the nerve, for 30 min) in isoflurane-anesthetized mice enhanced the influx of $CD45^+$ immune cells into BALF ($p \leq 0.05$; Fig. 1A), mucus metaplasia (Fig. 1B) and BALF mucin imbalance (Muc5AC/Muc5B; Fig. 1C). Optical stimulation did not affect goblet cell hyperplasia (Supplementary figure 1A)

in littermate control mice with no channelrhodopsin ($cre^{-/-}ChR2^{fl/wt}$; Fig. 1A-C) or in mice where only vagal autonomic neurons were activated (data not shown). Activation of vagal sensory neurons is sufficient, therefore, to trigger both immune cell influx into the lung and mucin imbalance. This article's Methods section is in the JACI Online Repository at www.jacionline.org.

Sensory neuron silencing strategy.

We exploited a nociceptor neuron blocking strategy to locally silence lung-innervating nociceptors and probe their role in driving pathological mucous cell metaplasia in allergic lung inflammation. This protocol uses large pore ion channels such as TRPV1, as cell-specific drug-entry ports that deliver a charged and membrane-impermeable form of lidocaine (QX-314) into sensory fibers to block sodium currents. During allergic airway inflammation, these ion channels on the surface of nociceptors open, allowing the small-size (263 Da) QX-314 to permeate into these neurons (6). This results in a highly targeted and long-lasting (>9h) electrical blockade of nociceptors, greatly exceeding efficacy of lidocaine (<1h). While QX-314 does not impact BALF immune cell function it reverses OVA-induced airway inflammation for up to 72h (6).

Sensory neuron-induced Muc5AC overproduction is independent of immune cells.

Mucin production and hypersecretion are influenced by inflammatory conditions, with immunocyte-produced cytokines modulating switches in mucin production (1). To test whether the effect of sensory neurons on mucin production is mediated directly or indirectly via airway-infiltrating leukocytes, we compared the effect of capsaicin-mediated activation of $TRPV1^{+}$ lung sensory neurons on mucin production in wildtype and in adaptive immune cell deficient mice ($Rag1^{-/-}$). Both wildtype and $Rag1^{-/-}$ mice treated with inhaled capsaicin to activate $TRPV1^{+}$ sensory neurons, present similar increases in BALF Muc5AC/Muc5B secreted levels (Fig. 1D) and goblet cell ($Muc2^{+}$) transcript expression of Muc5AC/Muc5B (Supplementary figure 1B). The effects of the capsaicin challenge were abolished when both sets of mice were co-treated with QX-314 (Fig. 1D, Supplementary figure 1B) which silences activity in these neurons by entry through activated large pore channels (6). Based on these results, we conclude that the sensory neuron-induced change in Muc5AC/Muc5B expression and release is independent of airway lymphocytes.

Sensory neurons control allergen-mediated mucin imbalance.

Mice were sensitized to ovalbumin (OVA) (intraperitoneally [i.p.] with aluminum hydroxide, days 0 and 7) as an allergen, followed by inhaled OVA challenges on days 14–17 (6). QX-314 (100 µM; 20 min aerosol; day 18) prevents the OVA-challenge induced mucus metaplasia (Fig 1E, J-L), and imbalance (Muc5AC/Muc5B) as well as the changes in transcribed mucins (Fig 1F-I; Supplementary figure 1C) measured on day 21. QX-314 inhalation had no effect when administered in non-inflamed conditions (Fig. 1E). These findings support sensory neuron silencing as a potential therapeutic strategy to reverse asthma-mediated mucin imbalance.

Sensory neuron-released SP drives goblet cell hyperplasia.

Substance P (SP) is a sensory neuropeptide which is increased in the sputum of asthmatic patients (7) and contributes to the neurogenic component of inflammation (8). Here, we found that the OVA-challenge increased BALF SP levels, in a manner that was prevented by sensory neuron silencing with QX-314 (Supplementary figure 2A); indicating that airway type 2 inflammation activates axonal terminal release of SP. Next, we explored if sensory neurons heighten tracheal mucus production in type 2 allergic lung inflammation via locally-secreted SP. To do this we engineered mice whose peptidergic and other sensory neurons are genetically ablated by expression of diphtheria toxin in TRPV1 lineage cells ($TRPV1^{cre/wt}::DTA^{fl/wt}$). The stable NK-1R agonist [Sar^{9}-Met-$(O2)^{11}$]-SP directly drives mucus secretion in wildtype mice tracheas, as does the TRPV1 agonist capsaicin and the acetylcholine receptor agonist carbachol (Supplementary figure 2B). However, capsaicin-induced mucus secretion was not observed in sensory neuron ablated ($TRPV1^{cre/wt}::DTA^{fl/wt}$) and Tac1 knockout (no SP) mice but the degree of carbachol-induced mucus secretion was similar between these mice and their littermate controls (Supplementary figure 2P). Of note, sensory neuron silencing with QX-314 also did not impact carbachol (100 µM, 30 min) induced mucus secretion from OVA-challenged mice trachea (Supplementary figure 2C). These data suggest that vagal sensory neuron-mediated mucus secretion in the inflamed mouse trachea depends on SP secretion.

The excessive mucus production seen in allergic asthma patients is the consequence of increased transdifferentiation of airway ciliated epithelial cells into mucin-producing goblet cells, a phenomenon known as goblet cell hyperplasia. These cells are often found near airway sensory neuron terminals and express receptors for various neuropeptides (9). To test the hypothesis that neurons drive goblet cell hyperplasia, we found that OVA-exposed littermate control mice develop goblet cells hyperplasia, detected by alcian blue histological staining, as compared to vehicle-treated mice (Fig. 2A-G).

Sensory neuron silenced (QX-314), sensory neuron ablated (TRPV1$^{cre/wt}$::DTA$^{fl/wt}$) or Tac1 knockout mice were protected from this effect (Fig. 2G). Daily intranasal injections of the NK-1R agonist [Sar^{9}-Met-(O2)^{11}]-SP to TRPV1$^{cre/wt}$::DTA$^{fl/wt}$ mice also partially rescued the goblet cells hyperplasia (Fig. 2A-G).

Relative to naïve animals, OVA-challenged control mice present with a significant increase in airway mucus deposition (Fig. 2H; Supplementary figure 2 E-I), as well as an increase in the BALF ratio of Muc5AC/Muc5B (Fig. 2I), *in situ* Muc5AC transcripts levels (Fig. 2J; Supplementary figure 2J-N) and the NK-1R^{+} goblet cell Muc5AC/Muc5B transcript ratio (Supplementary figure 2D). These effects were absent in Tac1$^{-/-}$ or TRPV1$^{cre/wt}$::DTA$^{fl/wt}$ mice (Fig. 2H-J) or blocked by sensory neuron silencing with QX-314 (Supplementary figure 2D). Daily intranasal injections of [Sar^{9}-Met-(O2)^{11}]-SP in TRPV1$^{cre/wt}$::DTA$^{fl/wt}$ mice increased these levels close to ones measured in mice with OVA-induced inflammation (Fig. 2H-J), supporting a direct role for SP in the changes.

Currently no therapies target the resolution of allergy-induced mucous cell metaplasia and hypersecretion of Muc5AC nor can rescue mucociliary transport in asthma, COPD or cystic fibrosis patients (3). Given the contribution that SP release from activated sensory neurons play in these changes, silencing these sensory neurons may constitute a viable treatment strategy for these pathologies.

Sébastien Talbot, *PhD* [a,b,c,*]
Benjamin Doyle, *MSc* [a,b]
Junwei Huang, *PhD* [a,b]
Jo-Chiao Wang, *MSc* [c]
Maryam Ahmadi, *MSc* [c]
David P. Roberson, *PhD* [a,b]
Ajay Yekkirala, *PhD* [a,b]
Simmie L. Foster, *MD, PhD* [a,b]
Liam E. Browne, *PhD* [a,b,e]
Bruce P. Bean, *PhD* [b]
Bruce D. Levy, *MD* [d]
Clifford J. Woolf, *MB, BCh, PhD* [a, b,*]

From [a]the FM Kirby Neurobiology Center, Children's Hospital Boston, Boston, USA; [b]the Department of Neurobiology, Harvard Medical School, Boston, USA; [c] the Département de Pharmacologie et Physiologie, Université de Montréal, Montréal, Canada; [d]the Pulmonary and Critical Care Medicine Division, Department of Internal Medicine, Brigham and Women's Hospital, Harvard Medical School, Boston, USA; and [e]the Wolfson Institute for Biomedical Research, University College London, London, UK.

Disclosure of potential conflict of interest: ST, DR, BPB, BDL and CJW have an equity stake in Nocion Therapeutics.

Acknowledgments. This work was partially supported by the National Institute of Health grants (CJW and BPB; PO1NS072040) and (BDL; HL122531); the Canadian Institutes of Health Research (ST), the Canada Research Chair program (ST), Natural Sciences and Engineering Research Council of Canada (ST) and the Brain Canada Foundation, Health Canada and the Azrieli Foundation (ST); as well as by a European Commission fellowship (LEB; 329202) and a Sir Henry Dale Fellowship jointly funded by the Wellcome Trust and the Royal Society (LEB; 109372/Z/15/Z). JCW received a Bastable-Potts Graduate research award from the Canadian Allergy, Asthma and Immunology Foundation.

Figure legends.

Figure 1. Airway sensory neuron neurons reverse mucus metaplasia and mucin imbalance. Optogenetic-stimulation of TRPV1$^{cre/wt}$::ChR2$^{fl/wt}$ and Tac1$^{cre/wt}$::ChR2$^{fl/wt}$ mice vagal sensory neurons increases BALF CD45^{+} cells (A), lung mucus deposition (B), and BALF Muc5AC/Muc5B ratio (C). In naïve C57BL6 mice, an acute capsaicin challenge (1 uM, i.n.) increased BALF levels of Muc5AC/Muc5B. Similar findings were observed in Rag1$^{-/-}$ mice, suggesting that these effects are independent of B or T cells. These consequences were absent when mice were co-treated with QX-314 (100 µM, intranasal, D) to silence sensory neurons. Allergen-challenges increased airway mucus deposition (E) as well as *in situ* expression of Muc5AC/Muc5B (F), effects that were reversed by sensory neuron silencing using QX-314 (100 uM, aerosolized). QX-314 had no detectable outcomes when given to naïve mice (E-F). Muc5AC (red) and Muc5B (green) transcript expression (G-I) visualized by *in situ*-hybridization-stained sections of naïve (G) and OVA-exposed (H, I) lungs treated with saline (G, I) or QX-314 (100 µM; H). Scale 100 µm. Mucus deposition (purple; J-L) in Periodic acid–Schiff-stained sections of naïve (J) and OVA-exposed (K, L) lungs treated with saline (J, K) or QX-314 (100 µM; L). DAPI-stained cell nucleus (blue; G-I). Scale 100 µm. Mean ± S.E.M; Two-tailed unpaired Student's t-test.

Figure 2: Allergic inflammation-mediated goblet cell hyperplasia and mucin imbalance are controlled by SP release from vagal sensory neurons. Goblet cell hyperplasia (blue; A-F) detected in Alcian Blue (AB)-stained sections of naïve (A) and OVA-exposed (B-F) lungs from littermate control (A-C), Tac1$^{-/-}$ (D), or sensory neuron ablated mice (E, F) treated with vehicle (A, B, D, E), QX-314 (100 uM; C) or [Sar^{9}, Met(O2)^{11}]-SP (F). Scale 100 µm. Littermate control mice challenged with OVA present a significant goblet cell hyperplasia (G), mucus metaplasia (H), BALF Muc5AC/Muc5B levels (I) as well as *in situ* expression of Muc5AC (J) relative to naïve mice. These effects were absent in sensory neuron silenced (G), ablated (G-I) or Tac1 knockout (G-I) mice, but partially rescued by daily intranasal administration of the stable substance P analog Sar^{9}-Met-(O2)^{11}]-SP (G-I). Mean ± S.E.M; Two-tailed unpaired Student's t-test.

References

1. Fahy JV, Dickey BF. Airway mucus function and dysfunction. The New England journal of medicine. 2010;363(23):2233-47.

2. Voynow JA, Rubin BK. Mucins, mucus, and sputum. Chest. 2009;135(2):505-12.

3. Evans CM, Raclawska DS, Ttofali F, Liptzin DR, Fletcher AA, Harper DN, et al. The polymeric mucin Muc5ac is required for allergic airway hyperreactivity. Nature communications. 2015;6:6281.

4. Roy MG, Livraghi-Butrico A, Fletcher AA, McElwee MM, Evans SE, Boerner RM, et al. Muc5b is required for airway defence. Nature. 2014;505(7483):412-6.

5. Bando H, Nishio T, van der Horst GT, Masubuchi S, Hisa Y, Okamura H. Vagal regulation of respiratory clocks in mice. The Journal of neuroscience : the official journal of the Society for Neuroscience. 2007;27(16):4359-65.

6. Talbot S, Abdulnour RE, Burkett PR, Lee S, Cronin SJ, Pascal MA, et al. Silencing Nociceptor Neurons Reduces Allergic Airway Inflammation. Neuron. 2015;87(2):341-54.

7. Tomaki M, Ichinose M, Miura M, Hirayama Y, Yamauchi H, Nakajima N, et al. Elevated substance P content in induced sputum from patients with asthma and patients with chronic bronchitis. Am J Respir Crit Care Med. 1995;151(3 Pt 1):613-7.

8. Barnes PJ. Neurogenic inflammation and asthma. J Asthma. 1992;29(3):165-80.

9. Rogers DF. Motor control of airway goblet cells and glands. Respir Physiol. 2001;125(1-2):129-44.

Supplementary materials.

Online methods.

Ethics and animals.

All procedures were approved by the Institutional Animal Care and Use Committees of Boston Children's Hospital, Harvard Medical School and the Université de Montréal (CDEA #19027; #19028). 8-week old male and female mice were purchased from Jackson Laboratory and housed in standard environmental conditions (12h light/dark cycle; 23^{o}C; food and water ad libitum) at facilities accredited by the Association for Assessment and Accreditation of Laboratory Animal Care.

Mouse lines.

BALB/c (Stock No: 001026), Tac1$^{-/-}$ (B6.Cg-Tac1tm1Bbm/J; Stock No: 004103), Rag1$^{-/-}$ (B6.129S7-Rag1tm1Mom/J; Stock No: 002216), Tac1^{Cre} (B6;129S-Tac1tm1.1(cre)Hze/J; Stock No: 021877), DTA$^{fl/fl}$ (B6.129P2-Gt26Sortm1(DTA)Lky/J; Stock No: 009669), ChR2$^{fl/fl}$ (B6.Cg-Gt(ROSA)26Sortm27.1(CAG-COP4*H134R/tdTomato)Hze/J; Stock No: 012567), CHAT^{ChR2}-eYFP (B6.Cg-Tg(Chat-COP4*H134R/EYFP,Slc18a3)6Gfng/J; Stock No: 014546). We used the cre/lox toolbox to genetically-engineered the various mice lines used (TRPV1$^{cre/wt}$::DTA$^{fl/wt}$, TRPV1$^{cre/wt}$::ChR2$^{fl/wt}$, Tac1$^{cre/wt}$::ChR2$^{fl/wt}$ and littermate control) by crossing male heterozygote Cre mice to female homozygous loxP mice (1). All Cre driver lines used are viable and fertile and abnormal phenotypes were not detected. Offspring were tail clipped; tissue was used to assess the presence of transgene by standard PCR, as described by Jackson Laboratory. Offspring were used at 8 weeks of age.

Asthma model

Allergic airway inflammation was studied in an ovalbumin (OVA) based model (1, 2). On day 0 and 7, mice were sensitized by a 200 µl i.p. injections of a solution containing 1 mg/ml ovalbumin (Sigma-Aldrich) and 5 mg/ml aluminum hydroxide (Sigma-Aldrich, Boston, Ma). On day 14-17 (10:00 am) mice were exposed to 6% OVA aerosol for 25min to induce airways allergic inflammation. Drugs were nebulized on day 18 (10:00 am) and outcome assessed on day 21 (10:00 am).

Drugs

QX-314(1, 3) (Charged lidocaine derivative, Tocris #2313), Carbachol (muscarinic agonist; Sigma #PHR1511), [Sar^{9}, Met(O2)^{11}]-SP (NK1R stable agonist, Tocris # 1178) were diluted fresh in sterile PBS at various concentrations. Capsaicin (TRPV1 selective agonist, Sigma #M2028) was diluted in ethanol.

ELISA

Mice were anesthetized with urethane and a 20G sterile catheter inserted longitudinally into the trachea. 2 ml of ice-cold PBS with protease inhibitor cocktail (1x Sigma Fast Protease Inhibitor (Sigma #S8820) and 10µM epoxomicin (Enzo #BMLPI127100,), was injected into the lung, harvested and underwent a 400g centrifugation (15 min; 4^{o}C) (4). The cells were discarded. Samples were processed according to instruction using commercial ELISA kit specifically designed for substance P (5) (Phoenix Pharmaceuticals; catalog number EK-064-05), Muc5B (LSBio # LS-F22247), and Muc5AC (LSBio #LS-F4842). For SP ELISAs, BALF were concentrated to a final 200 µl volume following a 3h RT SpeedVac (Thermo Scientific; SpeedVac Concentrator, SPD1010) cycle (1).

Histology

Lungs were inflated to 20 cm H_2O with 1x zinc fixative (BD Pharmigen), the trachea was ligated, and lungs stored overnight in zinc fixative (RT, mild shaking). The lungs were then washed in PBS and serially immersed in 30, 50 and 70 % Ethanol solution (20 min/each solution; RT). Tissues were embedded in paraffin, serially cut at 4µm and stained with Alcian Blue (AB; Sigma #66011500MLF) to assess goblet cell hyperplasia (6) and with Periodic Acid Schiff (PAS; Abcam #ab150680) base solution to assess mucus deposition (7). Two blinded investigators scored 384 randomized/scrambled images per condition (6 zones/slide; 4 slides/animal and 3-4 animals/group). PAS scores range from 0 (absence of goblet cells) to 4 (extensive goblets cells in large and small diameter bronchioles). AB was scored using ImageJ has relative intensity (Arbitrary Unit) over background.

Immunofluorescence

Upon harvesting, inflated lungs were post-fixed overnight in 4% para-formaldehyde, wash in PBS and cryoprotected by sequential sucrose immersion (PBS 10-30% sucrose, Overnight). Sections were then mounted in O.C.T. (Tissue-tek), and serially cut in 20 µm coronal sections with a cryostat. The sections were thaw-mounted on Fisherbrad superfrost

microscopy slides and kept at -80°C. On the day of the experiment, sections were thawed at room temperature for 10 min. Sections were washed in PBS for 5 min, blocked for 1h at room temperature (PBS, 0.1% Triton X-100, 5% BSA) and exposed to the primary antibodies (Overnight, 4°C), namely rabbit anti-mouse Muc5B (Abcam # ab87376), mouse Anti-mouse Muc5AC (Thermofisher #MA5-12178). Other antibodies tested include anti-Muc5AC (Thermofisher #MA5-12178), anti-Muc5B (Abcam #ab77995), rabbit anti-mouse Muc5B (BioS USA #bs-2414R-A555), or rabbit anti-mouse Muc5AC (Novus #NBP2-15196AF405). Sections were then washed three times in PBS (5 min), exposed to the secondary antibodies (2h, dark), washed, coverslipped with vectashield with DAPI (Vector Labs #H-1200) and observed under fluorescent microscope (Nikon. Eclipse Ti2-U).

Fluorescent *in situ* hybridization.

Inflated lungs were post-fixed overnight in 4% para-formaldehyde, wash in PBS and cryoprotected by sequential sucrose immersion (PBS 10-30% sucrose, Overnight). Sections were mounted in O.C.T. (Tissue-tek), and serially cut in 20 µm coronal sections with a cryostat. The sections were thaw-mounted on fisherbrad superfrost microscopy slides and kept at -80°C. On the day of the experiment, sections were thawed at room temperature for 10 min. Fluorescent in situ hybridization was performed as described using the RNAscope® Fluorescent Multiplex Reagent Kit (ACD Bio #320850) The primary probes used to stain Muc5B was Mm-Muc5b (ACD Bio #471991) (8) and for Muc5AC was Mm-Muc5ac-C2 (ACD Bio #448471-C2)were used as described in the instruction (9). Sections were washed in PBS (5 min), coverslipped with Vectashield with DAPI (Vector Labs #H-1200) and observed under fluorescent microscope (Nikon. Eclipse Ti2-U).

Flow cytometry

Lungs were gently lavages with PBS, harvested, digested and single cells resuspended in FACS buffer (PBS, 2% FCS, EDTA), and incubated with Fc block (0.5 mg/ml, 10 min; BD Biosciences). Cells were then stained with monoclonal antibodies (FITC anti-mouse CD45, BD Biosciences, cat no: 553079; Cy7 anti-mouse NK1R (10), Novus, NB300-119APCCY7; Dylight350 anti-mouse Muc2, Novus, NB120-11197UV; 45 min, 4°C on ice). 10^4- 10^5 $CD45^-Muc2^+$ or $CD45^-NK1R^+$ cells were isolated using a BD FACSAria™ III sorter (BD Biosciences) directly in Qiazol for subsequent qPCR measurement.

SYBR green-based quantitative real-time PCR.

RNA was extracted from whole lungs or FACS-sorted $Muc2^+$ or $NK1R^+$ lung cells using Qiazol reagent, followed by the RNeasy mini kit (Qiagen, MD). DNase I treatment (Qiagen) was used to remove genomic DNA, and complementary DNA reverse transcribed using Superscript III with random hexamers (Life Technologies). For qPCR, cDNA was subjected to 2-step thermocycling using fast SYBR green master mix (Life Technologies), and data collection performed on an Applied Biosystems 7500 machine (Life Technologies) (1). Expression levels were normalized to β-actin using the ΔΔcT method. The following primers were used: β-actin forward (TCG TAC CAC AGG CAT TGT GAT GGA) (1), β-actin reverse (TGA TGT CAC GCA CGA TTT CCC TCT) (1), Muc5b forward (CTG GCA CCT GCT CTG TGC A) (11), Muc5b reverse (CAC TGC TTT GAG GCA GTT CT) (11), Muc5AC forward (ACC ACT TTC TCC TTC TCC ACA) (11), and Muc5AC reverse (ATG GAT GTT AGC CGT CCT G) (11).

Tracheal mucus secretion

Upon euthanasia, mice tracheas were dissected and placed in ice-cold Krebs–Ringer bicarbonate buffer. The trachea was cut dorsally along its length and placed in a custom-built chamber mucosal side up so that the serosal side was bathed in ~60 µl Ringers, and the mucosal side was exposed to air (12). The luminal surface was gently cleaned with absorbent paper, dried with a stream of air, and coated with ~5 µl of mineral oil (Sigma #M5904). The luminal surface was not cleaned with absorbent paper during the experiments involving capsaicin or [Sar^9, $Met(O2)^{11}$]-SP to avoid tissue damage that might trigger nociceptive responses. Pharmacological agents (100µM Carbachol, 10µM capsaicin, 100µM QX-314, 100µM [Sar^9, $Met(O2)^{11}$]-SP) (13) were added to the serosal side and images of droplets taken at 1s intervals using a digital camera (Nikon. Ti2-U) and analyzed using ImageJ (12). Secretion volumes were calculated using the formula $V=1.3\pi r^3$, where r is the radius (12). To be included in the analysis, each droplet had to meet the following criteria: (a) a circular outline, so that it could be assumed to be spherical; (b) clear edges, to allow accurate measurement of the radius; and (c) no fusion with neighboring droplets. Viability was tested at the end of each experiment by measuring the response to carbachol, and those glands that did not respond to carbachol (<5% of total) were excluded from the analysis (12). Secretion rates were calculated as the slopes of cumulative volume vs. time plots after fitting at least three data points by linear regression (r2>0.8, rates in nanoliter per minute per gland) (12).

Vagus nerve optogenetic

Animals were deeply anesthetized (isoflurane, 1.5%–2%, Abbott Laboratory), freely breathing, and maintained at normal body temperature. The left nodose/jugular complex was surgically exposed and an optic fiber (0.39 NA fiber, Thorlabs)

was coupled to a DPSS laser light source (473 nm, 100 mW, Ultralaser) was placed 5-10 mm from the nerve (14). Focal illumination was performed beneath the ganglion and above the pharyngeal and superior laryngeal branches of the left nodose/jugular complex (14). Thirty-minute light stimulation were as follow: 3.5 ms, 5Hz, 100 mW, which give approx. 2-6 mW/mm^2 of power on the nerve, was controlled by a shutter system (Uniblitz) (15).

Statistics

Data expressed as mean ± S.E.M. Statistical significance determined by two-tail unpaired Student's t-test. P values less than 0.05 were considered significant. Numbers of animals are defined in figures.

Online references.

1. Talbot S, Abdulnour RE, Burkett PR, Lee S, Cronin SJ, Pascal MA, et al. Silencing Nociceptor Neurons Reduces Allergic Airway Inflammation. Neuron. 2015;87(2):341-54.

2. Haworth O, Cernadas M, Yang R, Serhan CN, Levy BD. Resolvin E1 regulates interleukin 23, interferon-gamma and lipoxin A4 to promote the resolution of allergic airway inflammation. Nat Immunol. 2008;9(8):873-9.

3. Binshtok AM, Bean BP, Woolf CJ. Inhibition of nociceptors by TRPV1-mediated entry of impermeant sodium channel blockers. Nature. 2007;449(7162):607-10.

4. Krause T, Rockendorf N, Gaede KI, Ramaker K, Sinnecker H, Frey A. Validation of antibody reagents for mucin analysis in chronic inflammatory airway diseases. MAbs. 2017;9(2):333-41.

5. Herberth G, Daegelmann C, Weber A, Roder S, Giese T, Kramer U, et al. Association of neuropeptides with Th1/Th2 balance and allergic sensitization in children. Clin Exp Allergy. 2006;36(11):1408-16.

6. Temann UA, Geba GP, Rankin JA, Flavell RA. Expression of interleukin 9 in the lungs of transgenic mice causes airway inflammation, mast cell hyperplasia, and bronchial hyperresponsiveness. J Exp Med. 1998;188(7):1307-20.

7. Gu W, Zhang X, Yan Y, Wang Y, Huang L, Wang M, et al. B7-H3 participates in the development of Asthma by augmentation of the inflammatory response independent of TLR2 pathway. Sci Rep. 2017;7:40398.

8. Chen G, Sun L, Kato T, Okuda K, Martino MB, Abzhanova A, et al. IL-1beta dominates the promucin secretory cytokine profile in cystic fibrosis. J Clin Invest. 2019;129(10):4433-50.

9. Han S, Fink J, Jorg DJ, Lee E, Yum MK, Chatzeli L, et al. Defining the Identity and Dynamics of Adult Gastric Isthmus Stem Cells. Cell Stem Cell. 2019;25(3):342-56 e7.

10. Zhou Y, Wang M, Tong Y, Liu X, Zhang L, Dong D, et al. miR-206 Promotes Cancer Progression by Targeting Full-Length Neurokinin-1 Receptor in Breast Cancer. Technol Cancer Res Treat. 2019;18:1533033819875168.

11. Ehre C, Worthington EN, Liesman RM, Grubb BR, Barbier D, O'Neal WK, et al. Overexpressing mouse model demonstrates the protective role of Muc5ac in the lungs. Proc Natl Acad Sci U S A. 2012;109(41):16528-33.

12. Ianowski JP, Choi JY, Wine JJ, Hanrahan JW. Substance P stimulates CFTR-dependent fluid secretion by mouse tracheal submucosal glands. Pflugers Arch. 2008;457(2):529-37.

13. Talbot S, Chahmi E, Dias JP, Couture R. Key role for spinal dorsal horn microglial kinin B1 receptor in early diabetic pain neuropathy. J Neuroinflammation. 2010;7(1):36.

14. Chang RB, Strochlic DE, Williams EK, Umans BD, Liberles SD. Vagal Sensory Neuron Subtypes that Differentially Control Breathing. Cell. 2015;161(3):622-33.

15. Browne LE, Latremoliere A, Lehnert BP, Grantham A, Ward C, Alexandre C, et al. Time-Resolved Fast Mammalian Behavior Reveals the Complexity of Protective Pain Responses. Cell Rep. 2017;20(1):89-98.

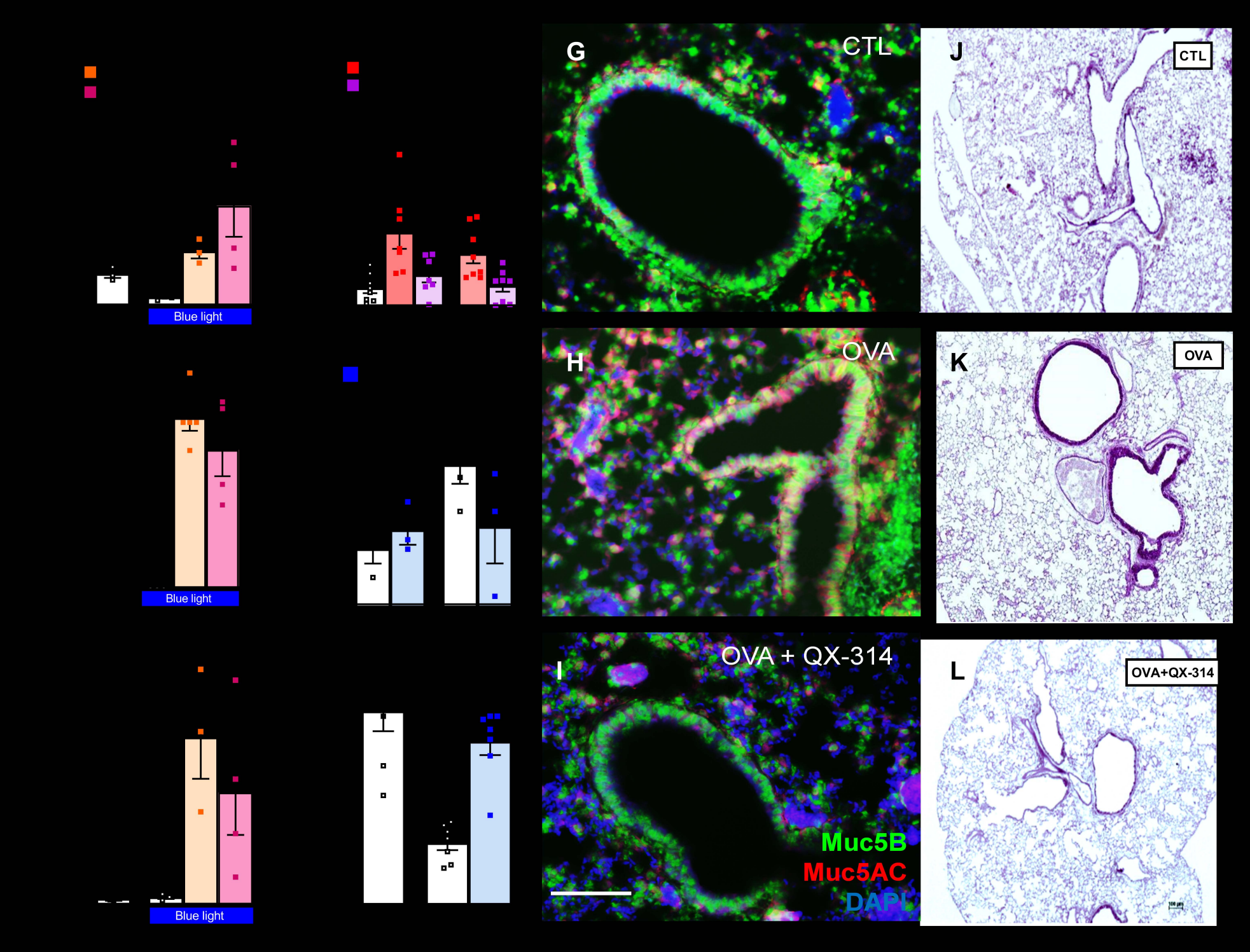
Blue light
Blue light
Blue light
G
CTL
H
OVA
I
OVA + QX-314
Muc5B
Muc5AC
DAPI
J
CTL
K
OVA
L
OVA+QX-314

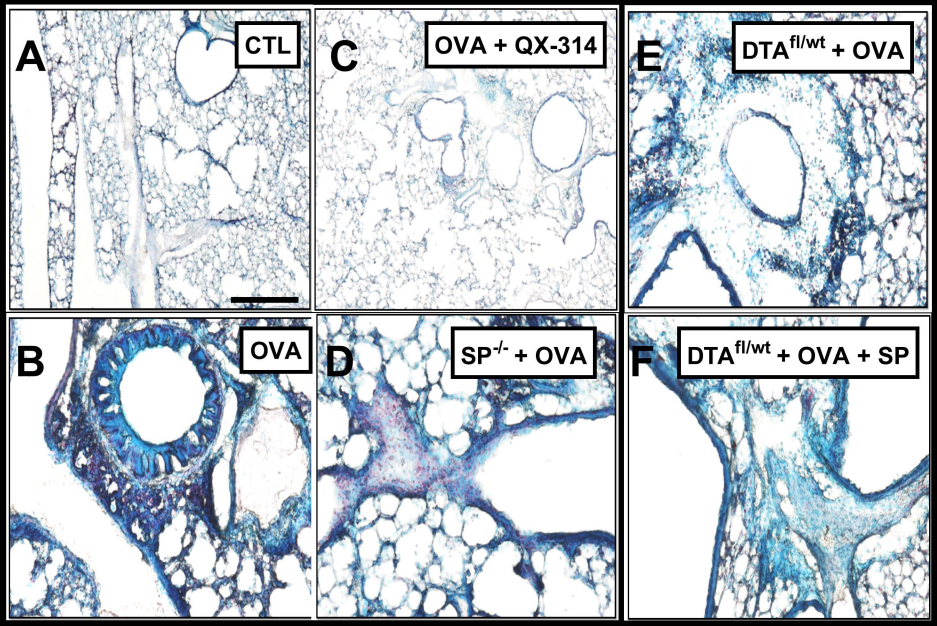
A
CTL
C
OVA + QX-314
E
DTA fl/wt + OVA
B
OVA
D
SP -/- + OVA
F
DTA fl/wt + OVA + SP

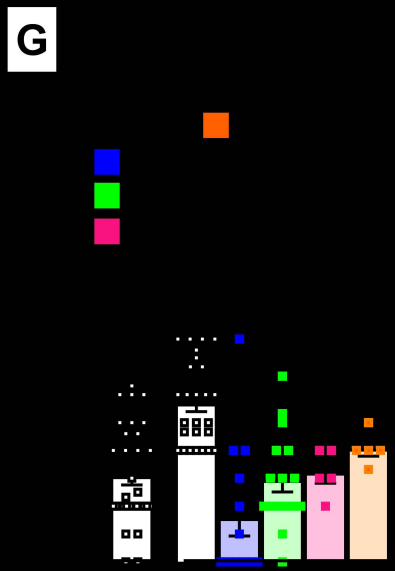
G

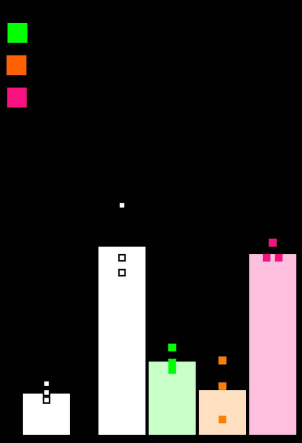

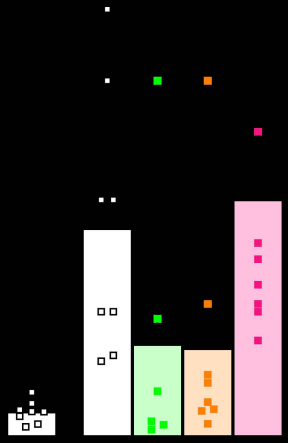

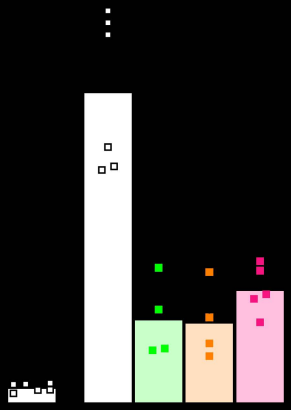

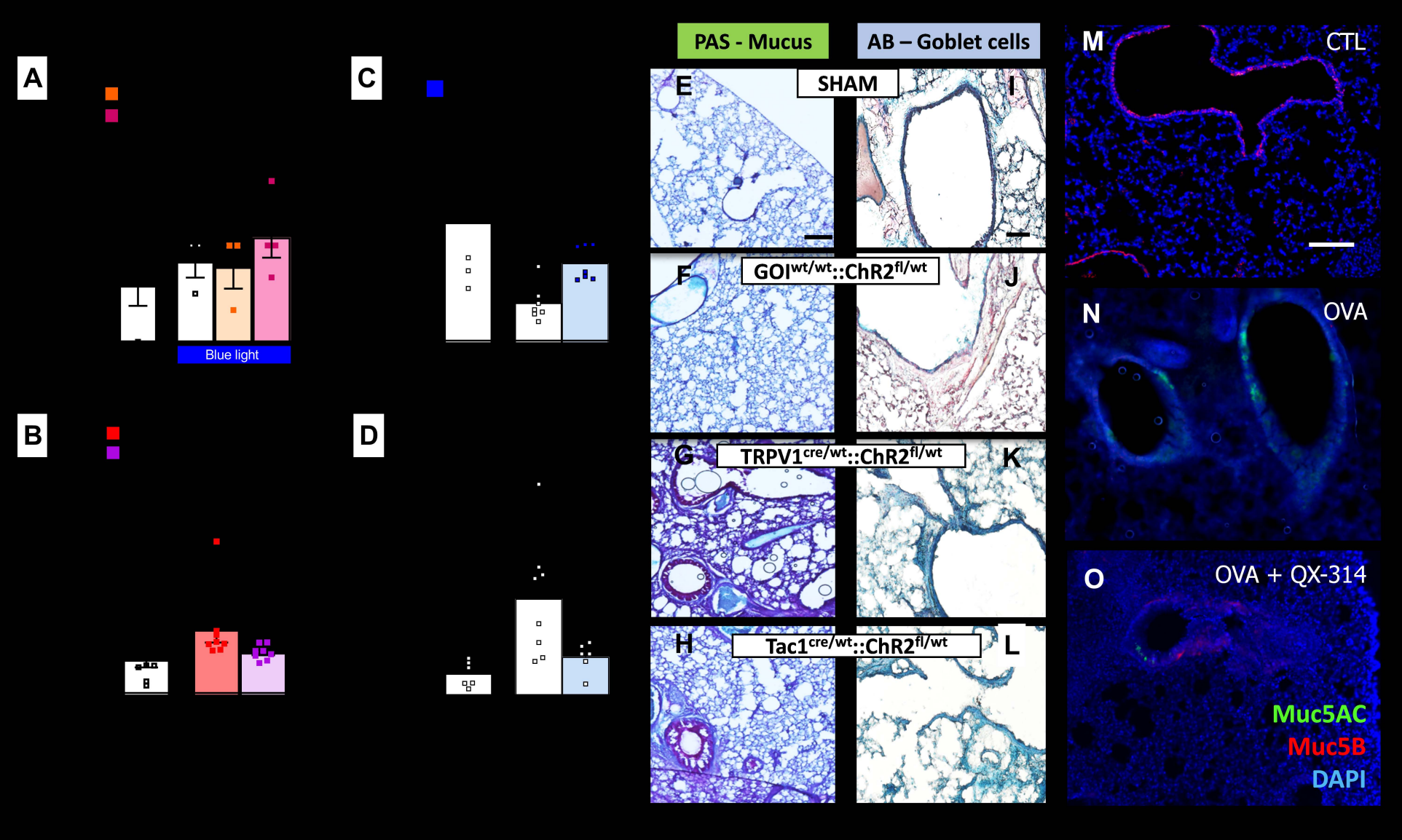
A
B
C
D
Blue light
PAS - Mucus
AB – Goblet cells
E
SHAM
I
F
GOI$^{wt/wt}$::ChR2$^{fl/wt}$
J
G
TRPV1$^{cre/wt}$::ChR2$^{fl/wt}$
K
H
Tac1$^{cre/wt}$::ChR2$^{fl/wt}$
L
M
CTL
N
OVA
O
OVA + QX-314
Muc5AC
Muc5B
DAPI

A
B
C
D
PAS - Mucus
In situ – Muc5AC
E
F
G
H
I
J
K
L
M
N
DAPI
Muc5AC
CTL
WT + OVA
DTA fl/wt + OVA
SP-/- + OVA
DTA fl/wt + OVA + SP

Supplementary figure legends.

Supplementary figure 1: Silencing sensory neuron neurons rescues allergen-mediated mucin imbalance. Optogenetic-stimulated (473nM, 5 Hz, 3.5 ms, 30 min, 100 mW) TRPV1$^{cre/wt}$::ChR2$^{fl/wt}$, Tac1$^{cre/wt}$::ChR2$^{fl/wt}$ and littermate control mice did not affect goblet cell hyperplasia (A). An acute capsaicin (1 uM, i.n.; B) or repeated allergen-challenges (C, D) increased airway goblet cell transcript expression (B, C) or BALF levels (D) of Muc5AC over Muc5B, these effects were reversed by sensory neuron silencing using QX-314 (100 uM; B-D). SHAM (E, I), and optogenetic-stimulated littermate control (F, J), TRPV1$^{cre/wt}$::ChR2$^{fl/wt}$ (G, K) and Tac1$^{cre/wt}$::ChR2$^{fl/wt}$ (H, L) mice lung section stained for mucus deposition (PAS, purple; E-H; Scale 100 µm) and goblet cell hyperplasia (AB, blue; I-L; Scale 30 µm). DAPI-stained cell nucleus (blue), Muc5B (red), Muc5AC (green)-stained sections of naïve (M) and OVA-exposed (N, O) lungs treated with saline (M, N) or QX-314 (100 µM; O). Scale 30 µm. Mean ± S.E.M; Two-tailed unpaired Student's t-test.

Supplementary figure 2: Sensory neuron silencing blocks SP release. OVA-challenge increased BALF Substance P, an effect prevented by sensory neuron silencing with QX-314 (100 µM, nebulized) (A). The TRPV1 agonist capsaicin (10 µM, 5 min), the stable NK-1R agonist [Sar^{9}-Met-(O2)^{11}]-SP (100 µM, 5 min) and carbachol (100 µM, 30 min) induced mucus secretion from OVA-challenged mice trachea (B-C). Capsaicin had no effect when administered to TRPV1$^{cre/wt}$::DTA$^{fl/wt}$ or Tac1$^{-/-}$ mice (B). QX-314 co-treatment do not impact carbachol (100 µM, 30 min) induced mucus secretion from OVA-challenged mice trachea (C). OVA-challenge increased lung NK-1R^{+} goblet cells Muc5AC/Muc5B ratio, an effect prevented by sensory neuron silencing with QX-314 and absent in Tac1$^{-/-}$ mice (D). Representative periodic acid–Schiff (purple, E-I) and *Muc5ac in situ* hybridization staining (red, J-N) of naïve (E, J), OVA-challenge littermate control (F, K), OVA-challenge TRPV1$^{cre/wt}$::DTA$^{fl/wt}$ (G, L), OVA-challenged Tac1$^{-/-}$ (H, M) or OVA-challenge TRPV1$^{cre/wt}$::DTA$^{fl/wt}$ + [Sar^{9}, Met(O2)^{11}]-SP (I, N) mice lung. Scale of 70 µm (I) and 30 µm (N), respectively. Mean ± S.E.M; Two-tailed unpaired Student's t-test.